8. STRENGTH OF SOILS AND ROCKS

8.1 COMPRESSIVE STRENGTH

The strength of a material may be broadly defined as the ability of the material to resist imposed forces. If is often measured as the maximum stress the material can sustain under specified loading and boundary conditions. Since an understanding of the behaviour in tension of a material such as steel is of great importance, the tensile strength of that material is normally measured and is used to compare one steel with another. In the case of soil, attention has been directed more towards the measurement and use of the shear strength or shearing resistance than towards any other strength parameter. (Bishop, 1966). In the case of concrete, the compressive strength is the most commonly measured strength parameter and this is also true of rock specimens.

For the uniaxial or unconfined compressive strength test a right circular cylinder of the material is compressed between the platens of a testing machine as illustrated in Fig. 8.1. The compressive strength is then defined as the maximum load applied to crush the specimen divided by the cross-sectional area. Rock strength has been found to be size dependent because of the cracks and fissures that are often present in the material. This is illustrated from the results of tests on three rock types in Fig. 8.2. The size dependancy is also found to exist for stiff fissured clays, as illustrated in Fig. 8.3 for London clay. Rocks with parallel arrangements of minerals or joints have been found to be noticeably anisotropic (different strengths in different directions). This particularly applies to metamorphic rocks as illustrated in Fig. 8.4. Strength testing of rock is discussed further by Franklin and Dusseault (1989).

8.2 TENSILE STRENGTH

The tensile strength of soil is very low or negligible and in most analyses it is considered to be zero. In contrast a number of direct or indirect tensile strength tests are commonly carried out for rock. In a direct tensile strength test a cylindrical rock specimen is stressed along its axis by means of a tensile force. The tensile strength is then calculated as the failure tensile force divided by the cross-sectional area.

It has been found that a rock core will split along a diameter when loaded on its side in a compression machine. This is the basis of the Brazilian test which is an indirect method of measuring tensile strength. A rock specimen having a disc shape with diameter (d) and thickness (t) is loaded as illustrated in Fig. 8.5. If the failure load is P then the tensile strength (σ_t) is calculated from

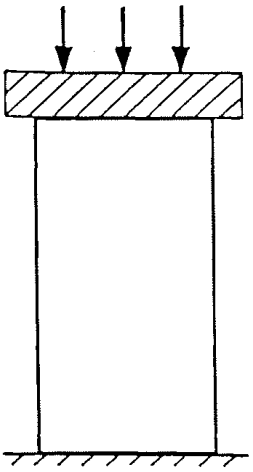

Fig. 8.1 Unconfined Compression Test

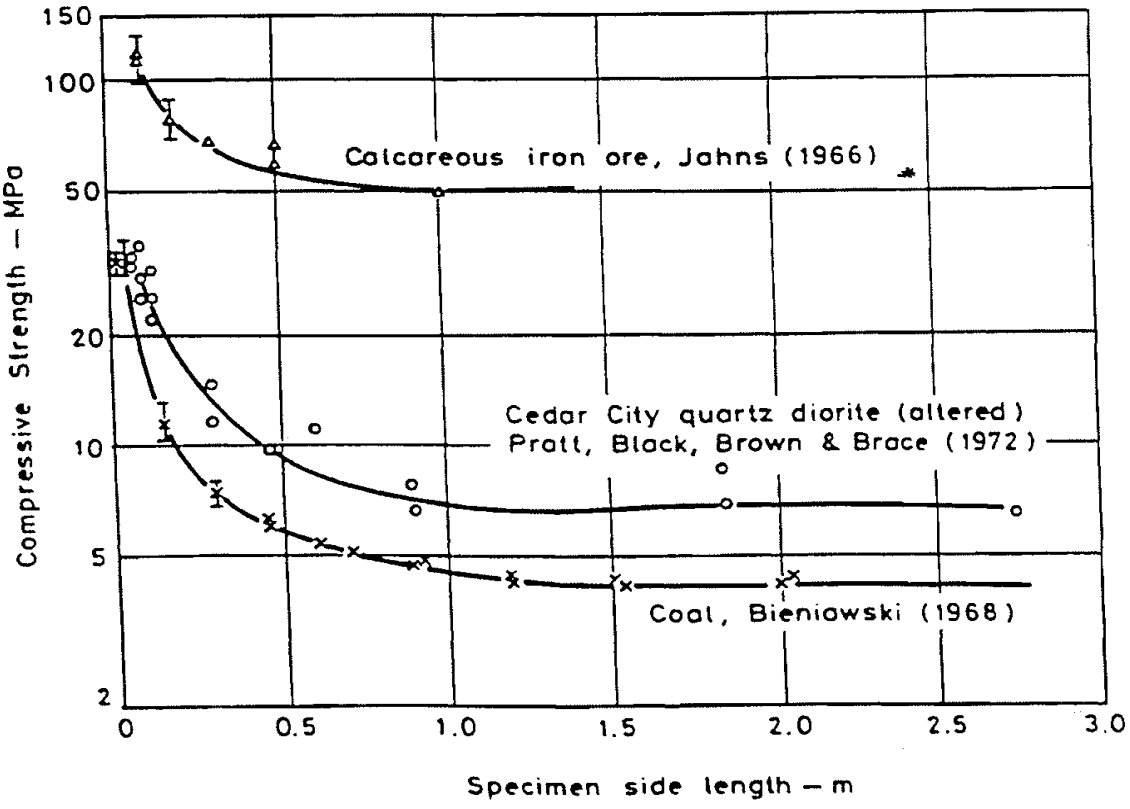

Fig. 8.2 Effect of Specimen Size on Unconfined Compressive Strength
(after Bieniawski & Van Heerden, 1975)

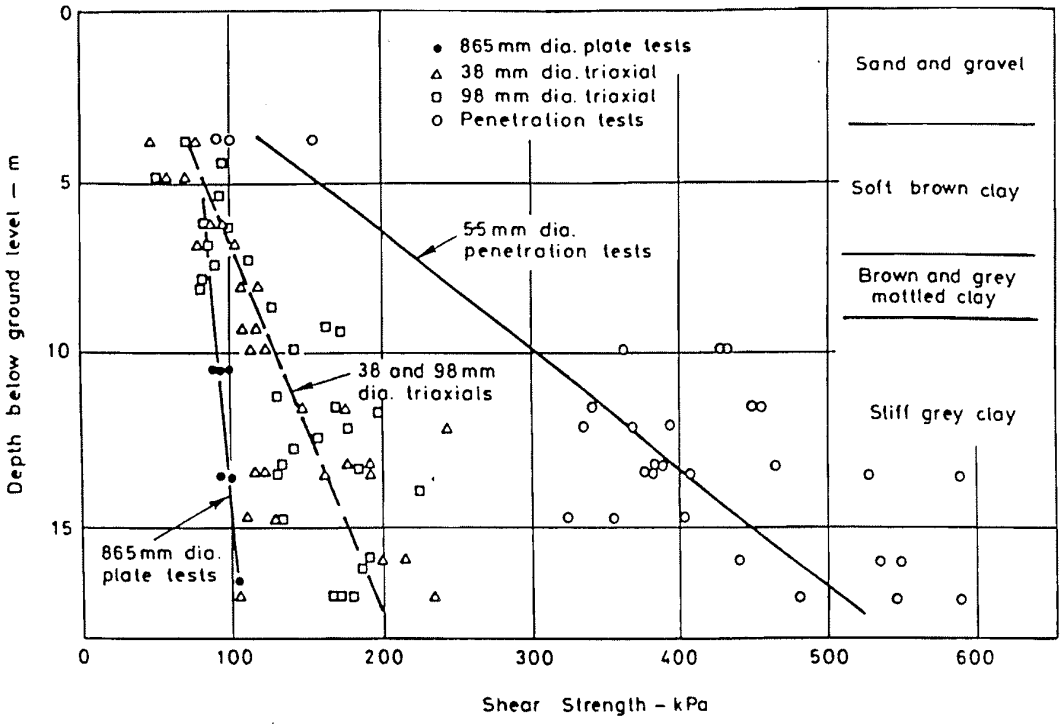

Fig. 8.3 Effect of Sample Size on Strength of London Clay (after Marsland, 1971)

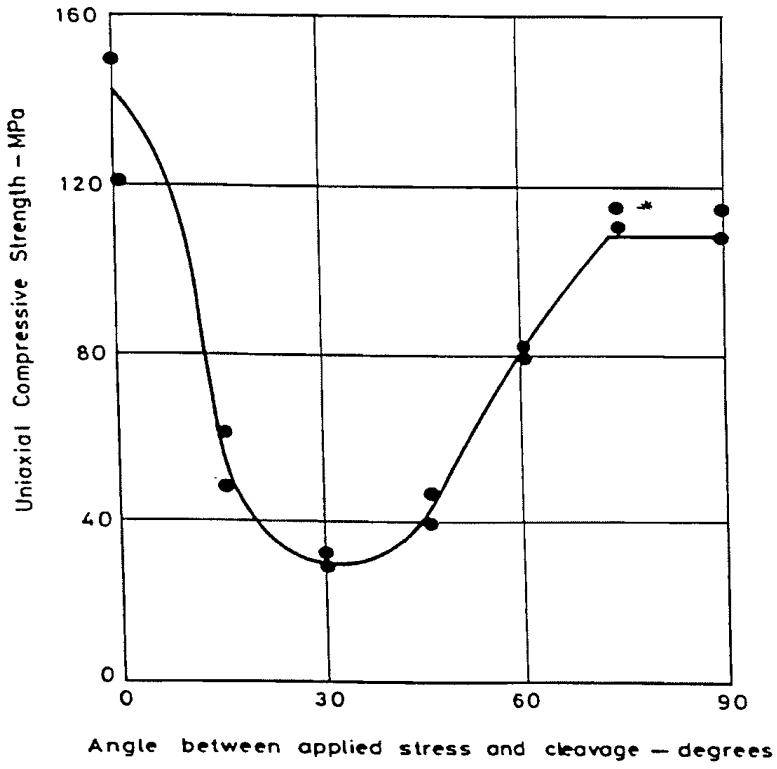

Fig. 8.4 Effect of Anisotropy on Strength of Slate
(after Franklin & Dusseault, 1989)

$$\sigma_t = 2P / (\pi d t) \quad (8.1)$$

Generally the Brazilian test is found to give a higher tensile strength than that obtained in a direct tension test, probably because of the effect of fissures in the rock.

Another method of determining tensile strength indirectly is by means of a flexural test in which a rock beam is failed by bending. Either three point or four point loading (Fig. 8.6) may be used in the test. For a cylindrical rock specimen (diameter d) and the four point loading arrangement as shown in Fig. 8.6, it may be shown that the tensile strength (σ_t) is

$$\sigma_t = 32 PL/(3\pi d^3) \quad (8.2)$$

where P is the failure load applied at each of the third points along the beam. For a beam of rectangular cross section (height h and width w) the tensile strength is

$$\sigma_t = 2 PL/(w h^2) \quad (8.3)$$

The tensile strength determined from beam bending tests is found to be two to three times the direct tensile strength.

The point load strength test may be used to provide an indirect measurement of tensile strength, but it is more commonly used as an index test. The point loading is applied to rock core specimens or to irregular rock fragments in a testing machine. If P is the failure load and D is the separation between the platens, the point load strength index (I_S) is defined as

$$I_S = P/D^2 \quad (8.4)$$

Corrections are applied to I_S to allow for specimen size and shape to yield the size corrected point load strength index (I_{S50}) which is defined as the value of I_S for a diametral test with D equal to 50mm. The value of I_{S50} is about 80% of the direct tensile strength.

8.3 SHEAR STRENGTH OF SOIL

One method of determination of the shearing resistance of a soil is similar to the procedure used to measure the coefficient of friction of a block sliding on a rough plane. This is illustrated in Fig. 8.7 which shows the results of a number of tests in which a block loaded by a normal force N is pulled by a shear force T until the block slides on the plane. The shear force required to cause sliding is indicated by T_{max}. The ratio of force T_{max} to force N, which is the slope of the line drawn through the plotted points is the coefficient of friction.

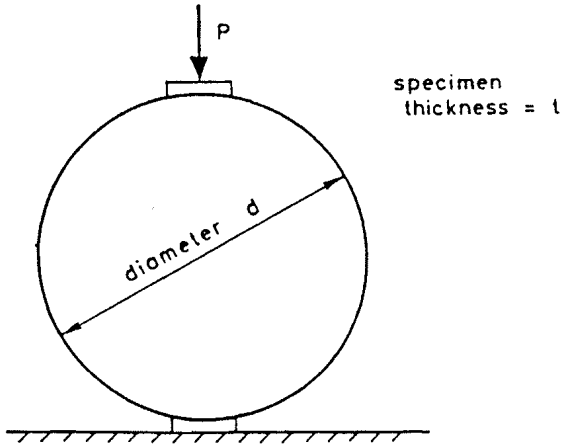

Fig. 8.5 Brazilian Test

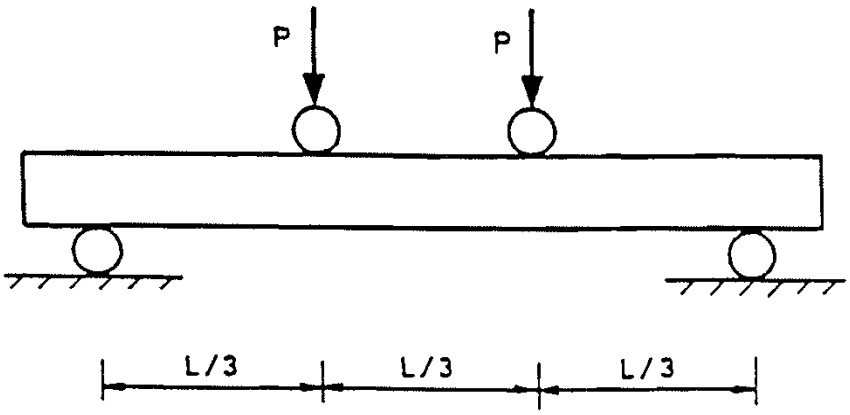

Fig. 8.6 Beam Bending Test

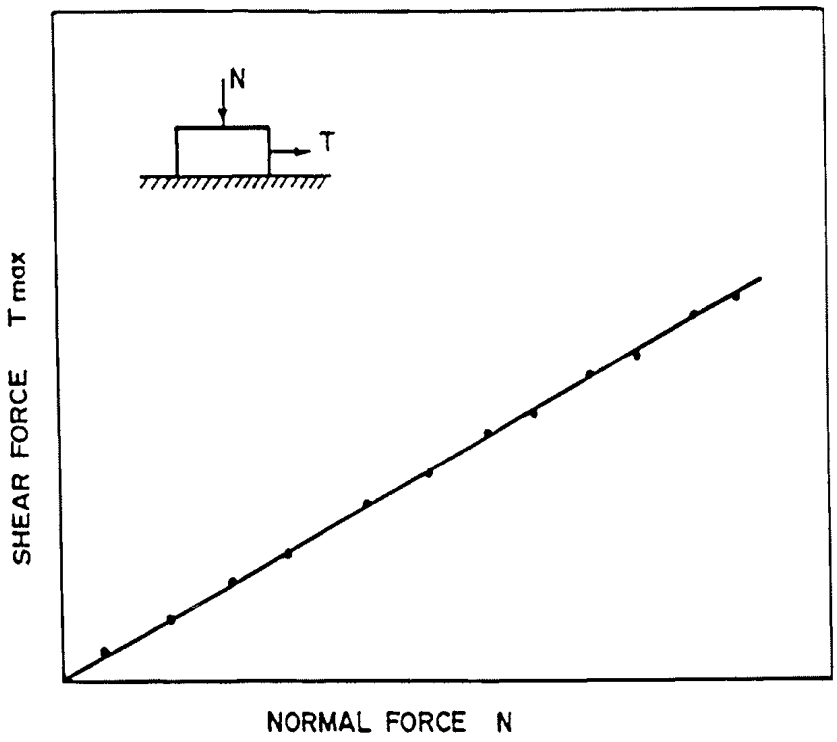

Fig. 8.7 Block Sliding on a Rough Plane

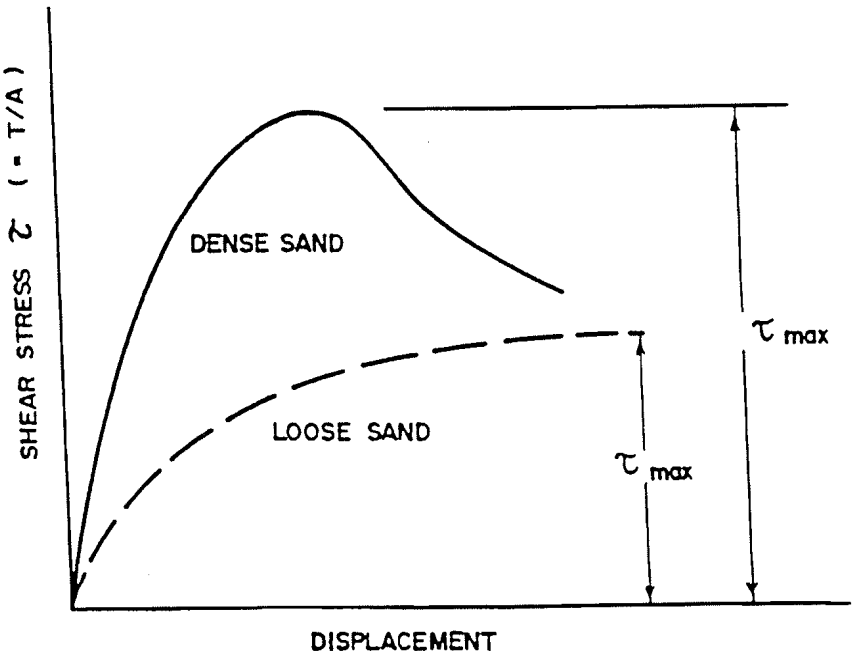

Fig. 8.8 Shear Stress - Diplacement Plots from Direct Shear Tests

The somewhat similar procedure that is used with soil is known as the direct shear test. For this test the soil sample is placed in a container in which one half can move relative to the other half thus imposing a shear stress on the sample. As the displacement in the direction of the shear force T of one half of the apparatus relative to the other half increases, the shear stress gradually builds up to a maximum value as illustrated in Fig. 8.8. The maximum value of the shear stress is the shear strength of the soil for the particular value of the normal force N or normal stress (N/A) applied to the soil, where A is the cross sectional area of the soil sample. Fig. 8.8 shows that a dense sand has a greater shear strength than a loose sand and this strength is reached at a smaller value of the displacement.

The results of a number of direct shear tests are shown in Fig. 8.9. The sand yields a shear stress-normal stress plot similar to that of the sliding block in Fig. 8.7 but the clay gives an intercept on the shear stress axis. The general equation of a straight line on this type of plot is

$$\tau_{max} = c + \sigma \tan \phi \qquad (8.5)$$

in which

c called the cohesion is the intercept on the shear stress axis

ϕ called the friction angle or angle of shearing resistance indicates the slope of the line.

Equation (8.5) is generally referred to as the Coulomb equation and this equation (the subscript max is often deleted) is commonly used to describe the strength of soils. The strength parameters c and ϕ may be expressed in terms of either total stresses or effective stresses. The lines (failure lines) plotted in Fig. 8.9 are straight but with many soils the lines exhibit a slight curvature. In these cases a straight line approximation over the relevant range of normal stress values is normally used.

It should be emphasised that a particular soil does not possess unique values of cohesion and friction angle. The values of the strength parameters c and ϕ depend upon the method of test as well as upon the soil type. Some of the commonly used methods of shear strength testing will be discussed in later sections of this chapter. Typical strength values for sands, silts and for rocks are given in Tables 8.1 and 8.2.

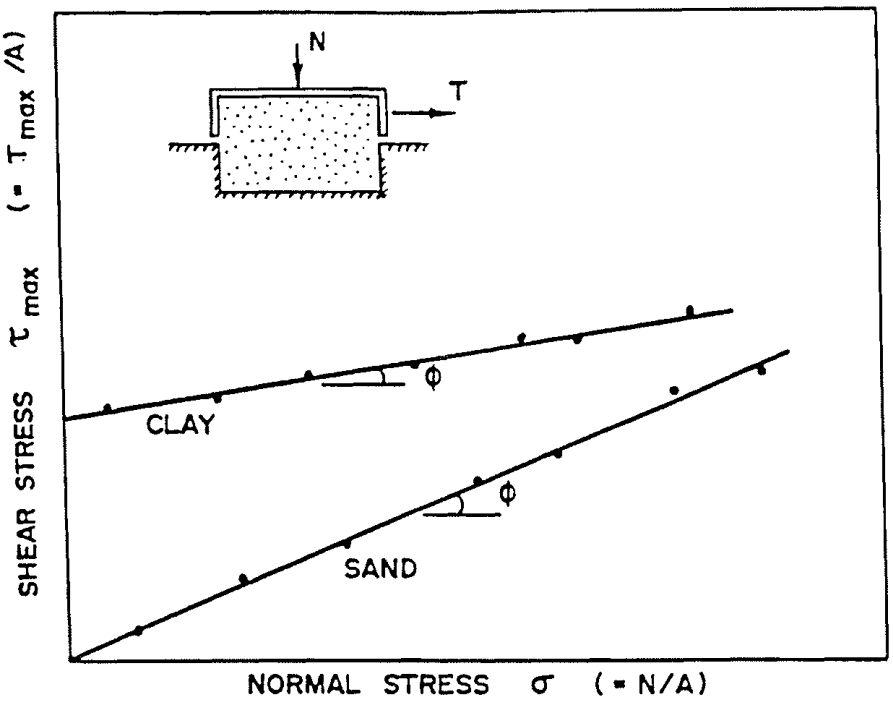

Fig. 8.9 Direct Shear Tests on Soils

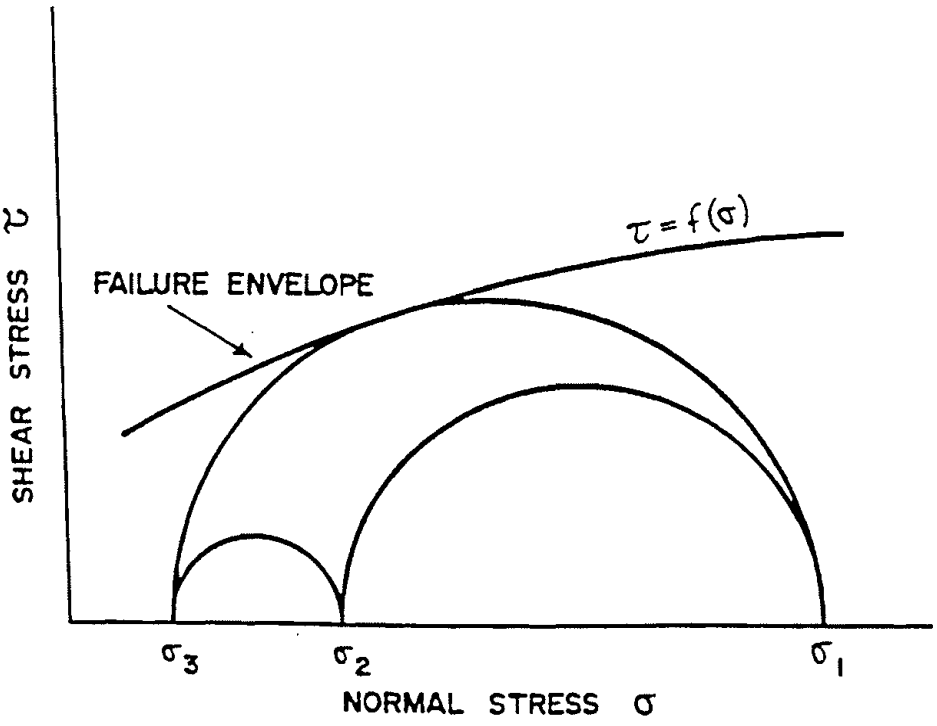

Fig. 8.10 Mohr Theory of Strength

TABLE 8.1

TYPICAL VALUES OF FRICTION ANGLE FOR SANDS AND SILTS
(after Terzaghi and Peck, 1967)

Material	Friction Angle (degrees)
Sand, uniform, round grains	27 - 34
Sand, well graded, angular	33 - 45
Sandy gravels	35 - 50
Silty sand	27 - 34
Inorganic silt	27 - 35

TABLE 8.2

TYPICAL STRENGTH VALUES FOR ROCKS
(after Goodman, 1980)

Rock	Cohesion (MPa)	Friction Angle (degrees)	Range of Confining Pressure (MPa)
Berea sandstone	27.2	27.8	0 - 200
Muddy shale	38.4	14.4	0 - 200
Sioux quartizite	70.6	48.0	0 - 203
Georgia marble	21.2	25.3	6 - 69
Chalk	0	31.5	10 - 90
Stone Mt. granite	55.1	51.0	0 - 69
Indiana limestone	6.7	42.0	0 - 10

8.4 THEORY OF STRENGTH

Several theories of strength have been applied to soils and rocks but the most widely used is the Mohr-Coloumb theory. This is based upon a combination of the Mohr theory of strength and the Coulomb equation.

Referring to Fig. 8.10 the stresses on the failure plane of a material are related by means of a general expression.

$$\tau = f(\sigma)$$

As the stresses on the soil increase to take the soil closer to failure the three principal stress circles enlarge. When the largest principal stress circle is tangent ot the line $\tau = f(\sigma)$ failure occurs on the plane corresponding to the point of tangency (see section 7.1). The intermediate principal stress, σ_2 is ignored in this theory. The line $\tau = f(\sigma)$ is therefore the envelope of all of the largest principal stress circles and the points of tangency represent the values of τ and σ on the failure planes.

A special case of this Mohr theory of strength is found when the failure envelope is a straight line as expressed by the Coulomb equation. This is the Mohr-Coulomb failure criterion which is commonly applied to soil and rock.

Fig. 8.11 gives a graphical representation of the Mohr-Coulomb failure criterion. From triangle PQR

$$\sin\phi = \frac{QR}{PR} = \frac{(\sigma_1 - \sigma_3)/2}{(\sigma_1 + \sigma_3)/2 + c\cot\phi}$$

$$= \frac{\sigma_1 - \sigma_3}{\sigma_1 + \sigma_3 + 2c\cot\phi}$$

$$\therefore \quad (\sigma_1 - \sigma_3) = (\sigma_1 + \sigma_3)\sin\phi + 2c\cos\phi \qquad (8.6)$$

This is the general form of the Mohr-Coulomb failure criterion.

From the foregoing discussion it is clear that one technique for determining the strength parameters, c and ϕ for a soil consists of measuring experimentally the failure values of σ_1 for a range of values of σ_3., From this data the largest Mohr circles corresponding to failure can be drawn and from the straight line envelope to these circles the values of c and ϕ may be found.

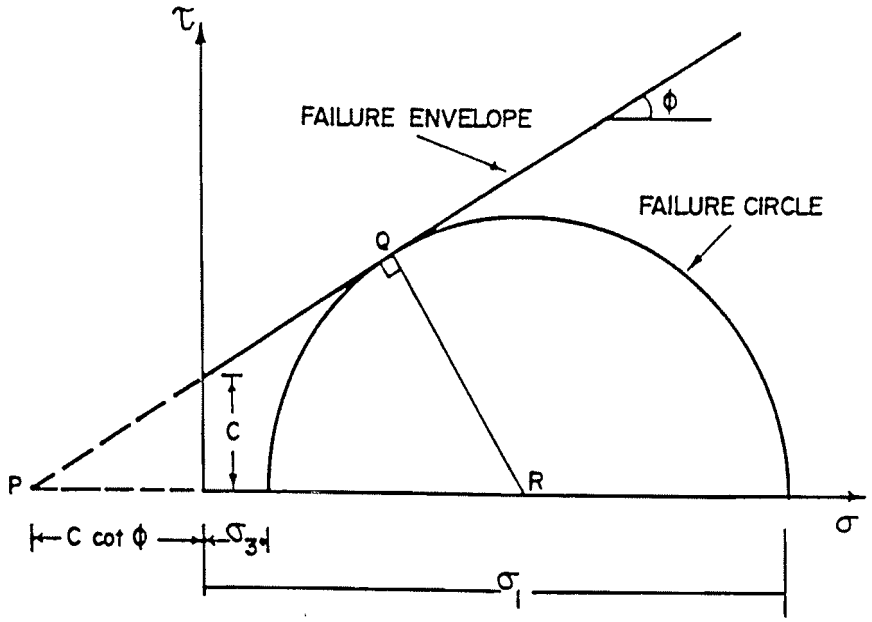

Fig. 8.11 Mohr - Coulomb Failure Criterion

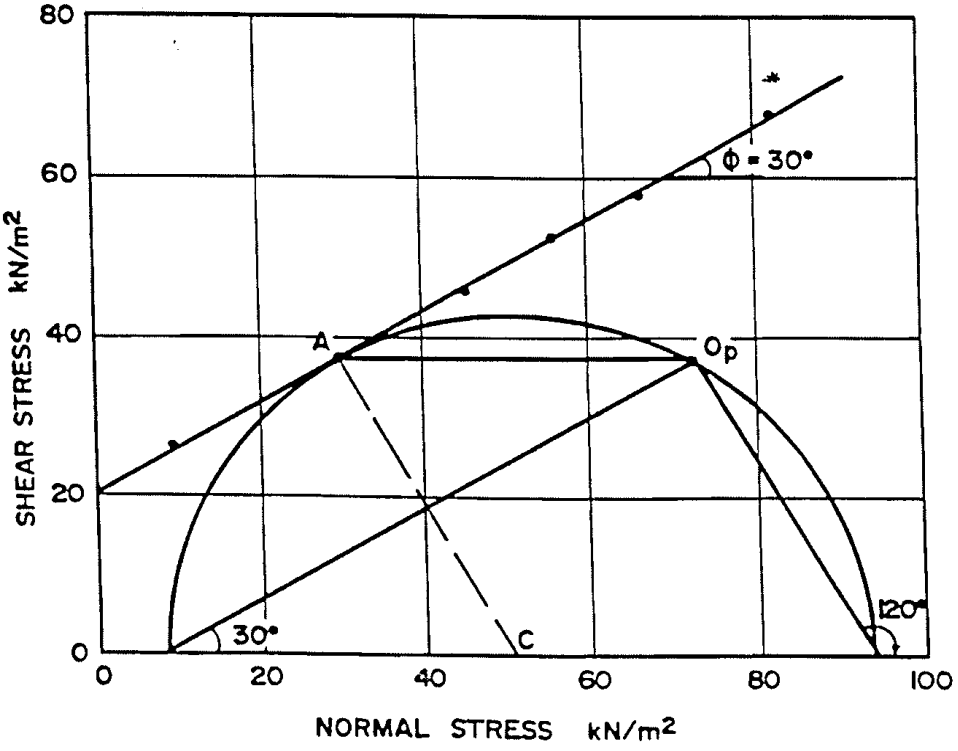

Fig. 8.12

EXAMPLE

The results of a number of direct shear tests on samples of a soil have been plotted in Fig. 8.12. The line drawn through the points gave strength parameters of

$$c = 20\text{kN/m}^2 \quad \text{and } \phi = 30^\circ$$

For the test in which the shear stress at failure and the normal stress were 37kN/m^2 and 30kN/m^2 respectively (point A in Fig. 8.12) determine

(a) the magnitudes of the principal stresses at failure,

(b) the inclinations of the principal planes.

(a) The principal stresses may be found by solving equations (7.1) and (7.2) to yield values of σ_1 and σ_3 of 94.1kN/m^2 and 8.6kN/m^2 respectively. In Fig. 8.12 the principal stresses have been determined by means of a much simpler though less precise graphical procedure. If a line AC is drawn from point A perpendicular to the failure line it will intersect the normal stress axis at the centre (C) of the failure Mohr circle. If this circle is drawn from centre C with CA as the radius the major and minor principal stresses may simply read from the diagram as 94kN/m^2 and 8.5kN/m^2 respectively.

(b) The inclinations of the principal planes may be found very easily by means of the origin of planes. In most direct shear tests the shear stress is applied horizontally and the failure plane must be horizontal. It will be assumed that this was the arrangement for the tests in this example.

With a horizontal failure plane the origin of planes, O_P may be located by drawing a horizontal line through the point (A) representing stresses on the failure plane. The inclinations of the principal planes may then be found by drawing lines from O_P to the points on the Mohr circle representing the principal stresses. This has been done in Fig. 8.12 which indicates that the major and minor principal planes are inclined to the horizontal by angles of 120° and 30° respectively.

8.5 EMPIRICAL FAILURE CRITERIA FOR ROCK

In contrast to the straight line failure envelope that is used with the Mohr-Coulomb failure criterion, Jaeger and Cook (1976) and Hoek (1968) have shown that the failure envelopes for most rocks lie between a straight line and a parabola. This has encouraged the development of empirical curve fitting methods to describe rock strength. Some of the empirical criteria that have been proposed are mentioned below.

Bieniawski (1974) has proposed the following empirical power law strength criterion

$$\frac{\sigma_1 - \sigma_3}{2\,\sigma_c} = 0.1 + B\left(\frac{\sigma_1 + \sigma_3}{2\sigma_c}\right)^a \qquad (8.7)$$

where σ_c = uniaxial compressive strength

a, B = constants to be evaluated.

The exponent a is typically in the range of 0.85 - 0.93. The constant B is usually within the range 0.7 - 0.8.

The Hoek and Brown (1980) criterion for rocks and rock masses is

$$\frac{\sigma_1}{\sigma_c} = \frac{\sigma_3}{\sigma_c} + \left(m\,\frac{\sigma_3}{\sigma_c} + s\right)^{1/2} \qquad (8.8)$$

where m and s and dimensionless parameters. The parameter m varies with rock type and ranges from 5.4 for limestone to 27.9 for granite. The parameter s varies from 1.0 for intact rock to zero for granular aggregates.

A better fit to experimental data may be obtained with the Yudhbir (1983) criterion which has three parameters A, B and a

$$\frac{\sigma_1}{\sigma_c} = A + B\left(\frac{\sigma_3}{\sigma_c}\right)^a \qquad (8.9)$$

A criterion proposed by Johnston (1985) to apply to a range of intact materials from clays to hard rocks for both compressive and tensile stress regions is

$$\frac{\sigma_1}{\sigma_c} = \left(\frac{M}{B}\,\frac{\sigma_3}{\sigma_c} + S\right)^B \qquad (8.10)$$

M and B are intact material constants. The constant S is an additional term to account for strength of discontinuous rock and rock masses. S = 1 for intact materials.

8.6 THE TRIAXIAL TEST

One of the disadvantages of the direct shear test is that the only stresses that are known throughout the performance of the test are the shear stress τ and normal stress σ on the failure plane. The magnitudes and directions of the principal stresses prior to failure are unknown. A further disadvantage of the direct shear test is that relatively little control over the drainage of water from the soil sample during testing is possible.

These disadvantages are overcome if the soil is tested in a laboratory device known as a triaxial cell. A cross section of such a cell is shown in Fig. 8.13. The cell facilitates axially symmetric loading on a cylindrical sample of soil. The confining pressure (usually σ_3) is provided by means of pressure applied to the water which is contained within the perspex cylinder and which surrounds the soil sample. The deviator stress ($\sigma_1 - \sigma_3$) is applied through the stainless steel ram and is measured by means of a proving ring or a force transducer. The drainage or pore pressure connection, as the name indicates, permits the test to be carried out under drained or undrained conditions. For the undrained test in which the water content of the soil is not allowed to change (see section 8.7) this connection is closed or it may be used for the measurement of pore pressure changes in the soil sample. For the drained test in which the pore pressure in the soil is not allowed to change, this connection is left open and the volume changes of a saturated sample may be monitored by measuring the volume of water expelled or taken in by the soil. Procedures to be followed in carrying out triaxial tests may be found in books on soil testing (Bishop and Henkel, 1962). Triaxial cells suitable for rock testing have been described by Vutukuri et al (1974) and by Brown (1981).

In the standard triaxial compression test the value of σ_3 is maintained constant and σ_1 (acting vertically) is increased until failure occurs. No independent control of the intermediate principal stress, σ_2, is possible in a triaxial test since $\sigma_2 = \sigma_3$. A typical stress-strain curve is shown in Fig. 8.14. The maximum value of ($\sigma_1 - \sigma_3$), which is the compressive strength of the soil for the particular value of σ_3 used in the test, is used as the diameter of the failure Mohr circle.

The failure circle has been drawn in Fig. 8.15(b). Since the major principal plane is horizontal the origin of planes, O_P is located on the left hand side of the circle. The inclination of the failure plane may be found by drawing a line from O_P to the point of tangency, A, with the failure envelope. From the geometry of the figure in Fig. 8.15(b) it may be demonstrated that the failure plane is inclined at an angle of $(45 + \phi/2)$ to the horizontal. The failure stress τ and σ on this failure plane shown in Fig. 8.15 (a) are represented by point A in Fig. 8.15 (b). Where any risk of confusion exists between τ and σ values on the failure plane at failure, on other planes at failure or on any plane prior to failure appropriate subscripts should be used.

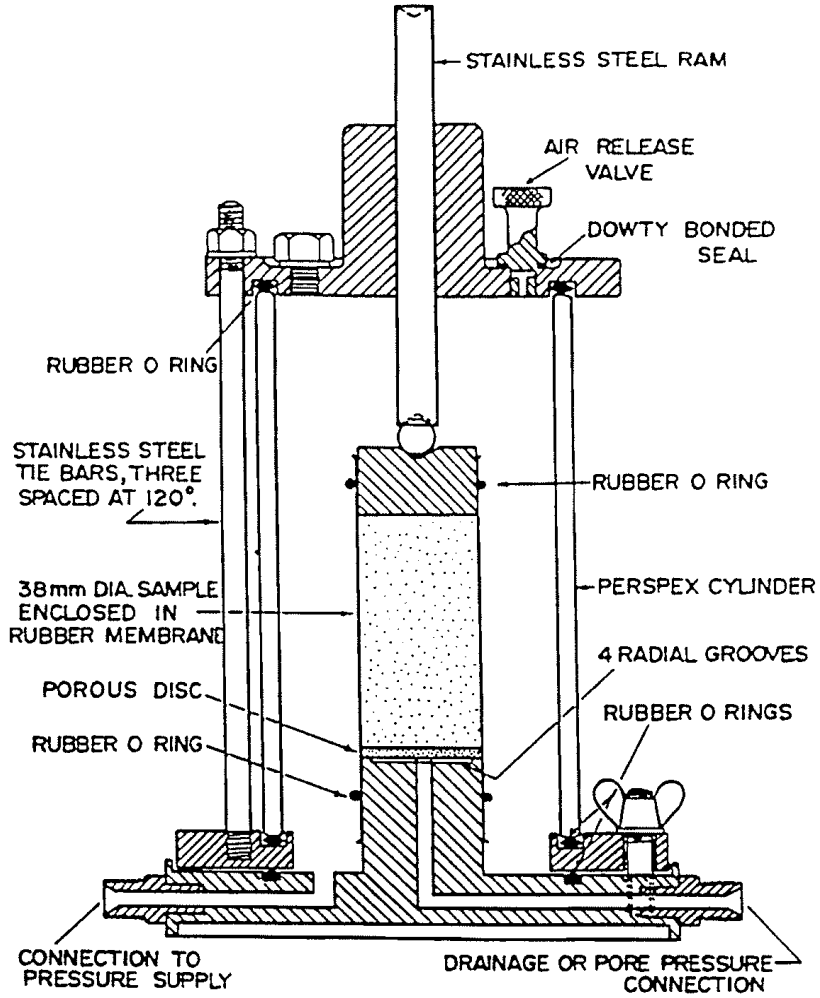

Fig. 8.13 Triaxial Cell

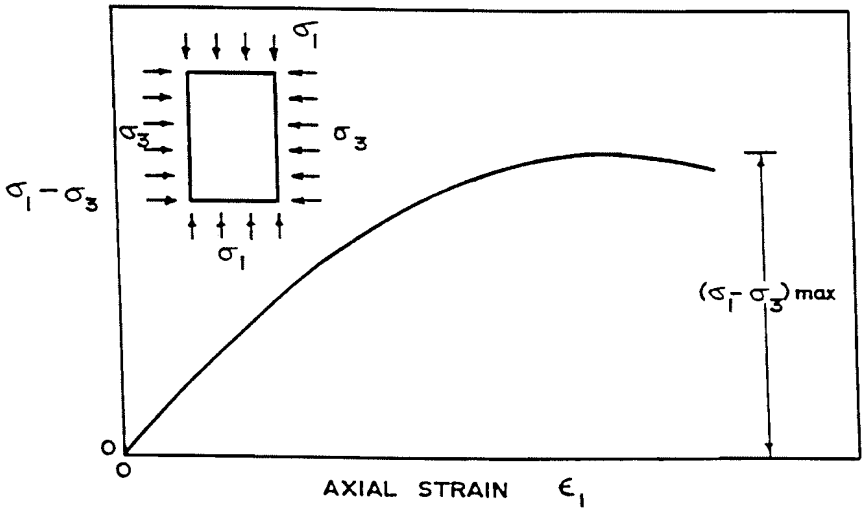

Fig. 8.14 Stress - Strain Curve for Axial Compression

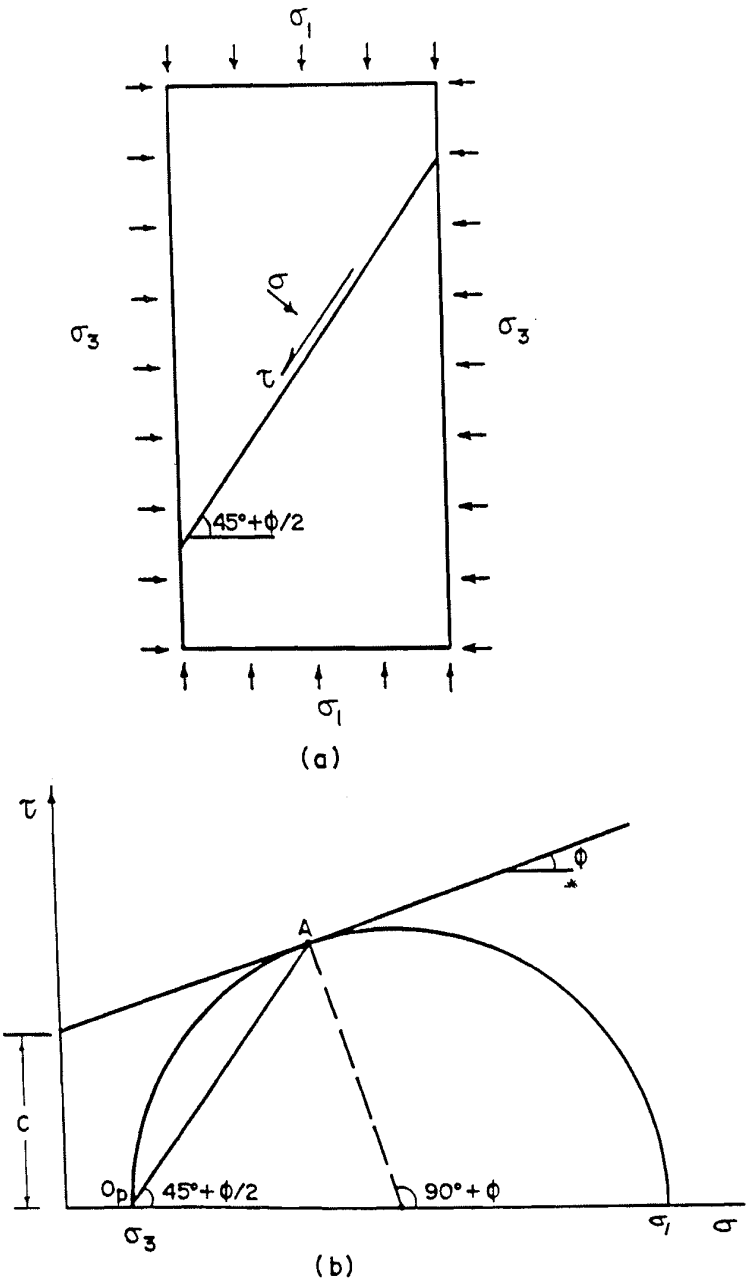

Fig. 8.15 Inclination of Failure Plane in a Triaxial Compression Test

The relationships between τ and σ on the failure plane at failure and the failure values of σ_1 and σ_3 may be found from the equations (7.1) and 7.2). If $(45 + \phi/2)$ is substituted for θ in these equations the following expressions are obtained.

$$\tau = \frac{(\sigma_1 - \sigma_3)}{2} \cos \phi \qquad (8.11)$$

$$\sigma = \frac{(\sigma_1 + \sigma_3)}{2} - \frac{(\sigma_1 - \sigma_3)}{2} \sin \phi \qquad (8.12)$$

Theoretically, if a direct shear test on a soil was conducted with a σ value given by equation (8.12) then, at failure a τ value given by equation (8.11) would be obtained.

Mohr circles and failure envelopes may be drawn for both total and effective stresses. Similarly the Coulomb equation may be expressed in terms of both total and effective stresses.

$$\tau = c + \sigma \tan \phi \qquad (8.13)$$

$$\tau = c' + \sigma' \tan \phi' \qquad (8.14)$$

Equation (8.13) is expressed in terms of total stresses and equation (8.14) is in terms of effective stresses. These two equations demonstrate the necessity of indicating whether strength parameters are in terms of total or effective stresses when values of c and ϕ are quoted (see Bishop and Bjerrum, 1960).

Further to the information given in Table 8.1, typical values of ϕ' for sandy soils may range from less than 30˚ for loose sands to more than 40˚ for dense sands. A typical value of c' for sandy soils is zero. For clay soils values of ϕ may range from zero for saturated soils (see section 8.7.3) to more than 40˚ for partly saturated soils. Values of ϕ' for clay soils typically range from 20˚ to 35˚. Values of c' for clay soils may range from zero for very soft or normally consolidated clay to more than 100kN/m^2 for stiff clay.

EXAMPLE

In an undrained triaxial compression test on a soil involving tests on three samples of the soil, each at a different value of σ_3, the following stresses at failure were measured

	σ_1 (kN/m^2)	σ_3 (kN/m^2)	u (kN/m^2)
(i)	135	65	50
(ii)	250	120	80
(iii)	400	200	125

Determine the strength parameters of the soil in terms of both total and effective stresses.

Using the values of σ_1 and σ_3 for tests (i), (ii) and (iii) the Mohr circles in terms of total stresses may be drawn as shown in Fig. 8.16 by the dashed lines. The straight line envelope to these three circles has been drawn and from this line the strength parameters may be read as

$c = 5\text{kN/m}^2$

$\phi = 19.0^\circ$

To plot the effective stress circles it is necessary to calculate σ_1' and σ_3'.

	σ_1' (kN/m^2)	σ_3' (kN/m^2)
(i)	135 - 50 = 85	65 - 50 = 15
(ii)	250 - 80 = 170	120 - 80 = 40
(iii)	400 - 125 = 275	200 - 125 = 75

With these stresses the effective Mohr circles have been drawn as the full lines in Fig. 8.16. The effective stress envelope to these circles yields the following strength parameters

$c' = 10\text{kN/m}^2$

$\phi' = 31.7^\circ$

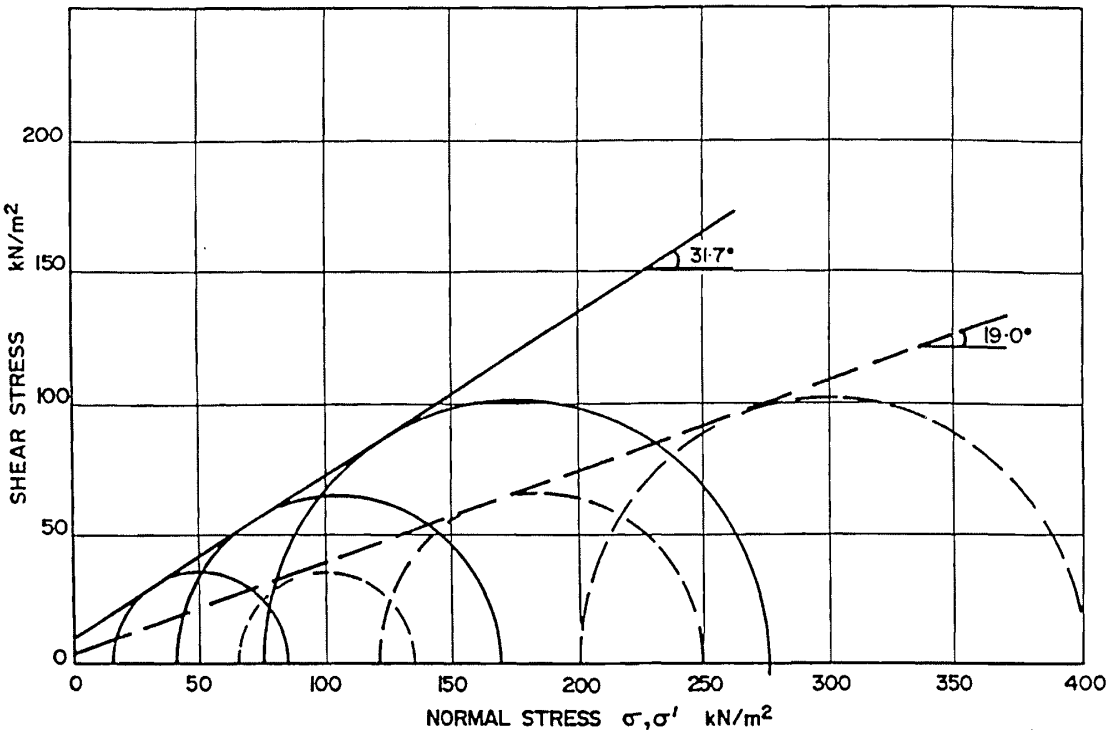

Fig. 8.16

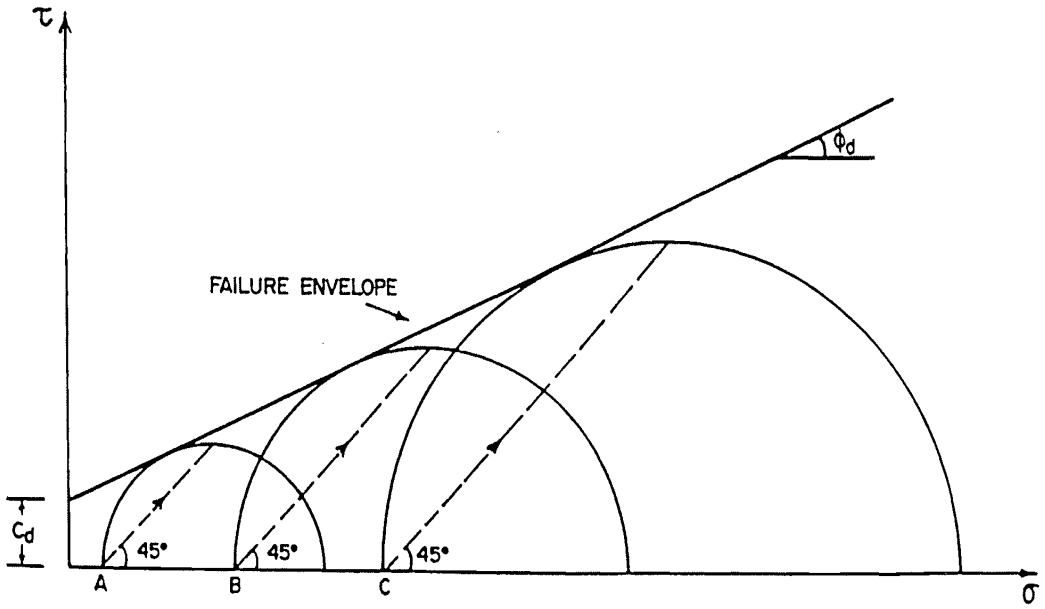

Fig. 8.17 Consolidated Drained Tests

8.7 EFFECT OF DRAINAGE UPON STRENGTH

In strength testing of soil, "drainage" refers to the provision of access to the soil of water outside of the soil, so that the soil may take in water or expel water in response to stresses applied to the soil. Drainage may be allowed or prevented at two stages during a routine triaxial compression test on a soil:

(i) During initial application of a confining pressure to the sample. If drainage is allowed then the soil will consolidate under the confining pressure. If drainage is prevented the soil will not consolidate and the shearing phase of the test will commence with an initial pore pressure in the soil. The magnitude of this initial pore pressure may be determined from equation (7.7).

(ii) During application of the deviator stress in the shearing phase of the test to produce failure of the sample. If drainage is allowed, that is, if the test is performed sufficiently slowly that any developed pore pressures are allowed to dissipate then a slow or drained test is performed. If drainage is prevented, that is, if any developed pore pressures are not allowed to dissipate then a quick or undrained test is performed.

8.7.1 The Consolidated Drained (CD) Test

This test is performed by initially consolidating a sample of soil then shearing it (by application of a deviator stress) under drained conditions. The results of three such tests on a soil are shown in Fig. 8.17. Points A, B and C represent the three consolidation stresses for each of the three samples. Since points A, B and C are located on the σ axis this means that the samples were consolidated isotropically. In other words for each sample the consolidation stresses in the three coordinate directions are equal; that is $\sigma_{1c}' = \sigma_{2c}' = \sigma_{3c}' (= \sigma_c')$. The stress paths (see section 7.2) to failure are shown by the dashed lines. These stress paths are both total stress paths and effective stress paths since pore pressures are being allowed to dissipate throughout the test. The failure envelope may be expressed as follows

$$\tau = c_d + \sigma \tan \phi_d \qquad (8.15)$$

where τ is the shear strength (shear stress on the failure plane at failure) for drained conditions

c_d is the drained cohesion

ϕ_d is the drained friction angle

The strength parameters c_d and ϕ_d may be applied to field problems in which the soil is loaded under drained conditions or in which the pore pressures developed during loading have fully dissipated. In other words the drained strength parameters are applicable to long term stability problems in the field (covered in later courses).

In Fig. 8.17 the ends of the three stress paths do not terminate on the failure envelope. As it is often convenient to represent failure on a q - p plot an alternative line representing failure has been drawn through the tops of the failure Mohr circles in Fig. 8.18. The general equation for this dashed line is

$$q = a + p \tan \alpha$$

which may be used with both total and effective stresses. If there is any risk of confusion with pre-failure values of q and p the equation is

$$q_f = a + p_f \tan \alpha \qquad (8.16)$$

where a and α are the alternative strength parameters. These values of a and α are uniquely related to the corresponding values of c and ϕ shown in Fig. 8.18. From the geometry of this figure it may be shown that

$$\sin \phi = \tan \alpha$$

$$c = a/\cos \phi \qquad (8.17)$$

If the foregoing equations are applied to the results of consolidated drained triaxial tests then the “d” subscript should be used on all strength parameters. If analysis is being carried out in terms of effective stresses then the ' superscript should be used on all parameters.

EXAMPLE

If the shear strength of a soil is expressed as

$$q_f = 10 + p_f \tan 30^\circ \text{ kN/m}^2$$

determine, (i) the inclination of the failure plane to the major principal plane, and (ii), the shear stress on the failure plane at failure for a normal stress (σ) of 50kN/m^2.

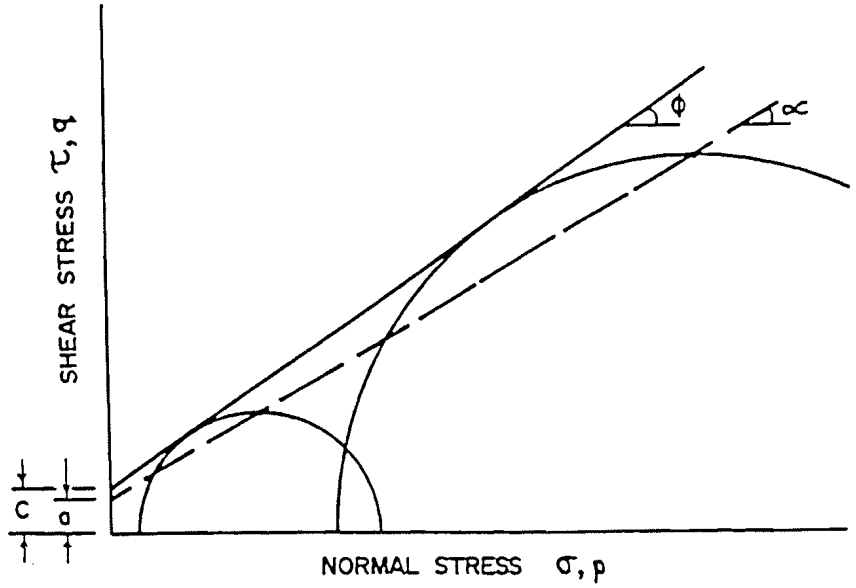

Fig. 8.18 Failure Line on a q-p Plot

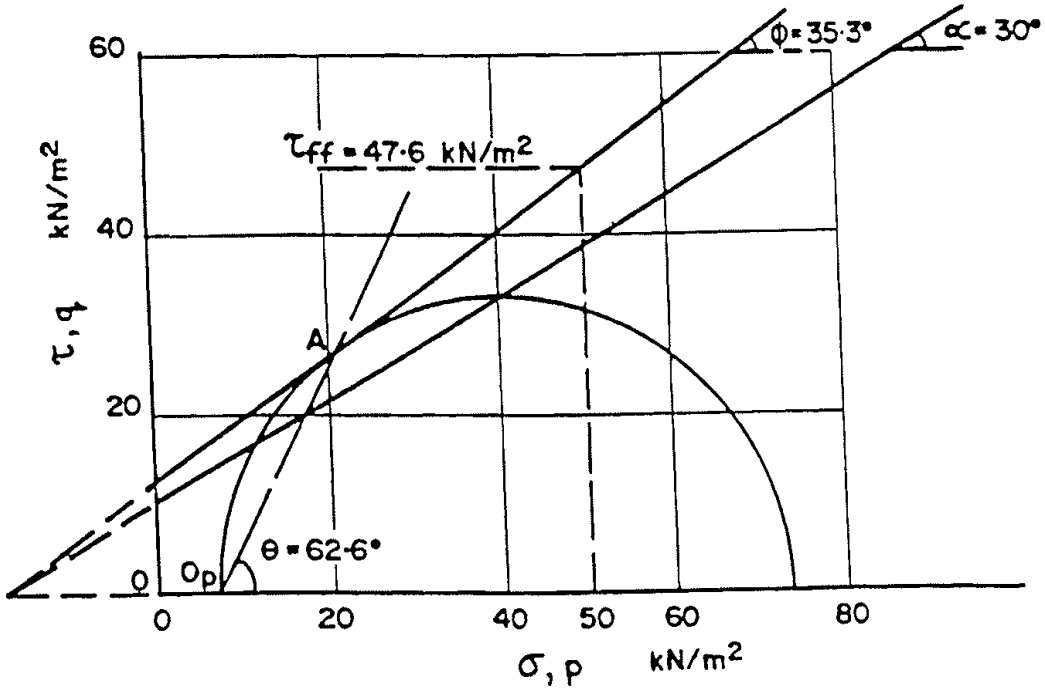

Fig. 8.19

(i) The failure line has been plotted on a q - p plot in Fig. 8.19. Since this failure line represents the locus of the tops of failure Mohr circles any such circle may be constructed as shown in the figure. From a knowledge of a and α, the values of c and ϕ may be calculated from equations (8.17) to enable the failure envelope ($\tau = c + \sigma \tan \phi$) to be drawn. Alternatively the failure envelope may be drawn from the geometry of Fig. 8.19. The point of tangency with the failure envelope (the point representing the stresses on the failure plane) is located at A.

If the major principal plane is horizontal the origin of planes is located at the left side of the circle. The failure plane is parallel to O_PA which has an inclination of 62.6° to the major principal plane. It should be noted that this answer is independent of the absolute direction of the major principal plane and it is independent of the particular failure circle chosen to find it.

(ii) The shear stress on the failure plane at failure may be calculated from a knowledge of the parameters c and ϕ

$$\tau_{ff} = c + \sigma_{ff} \tan \phi$$

$$= 12.2 + 50 \tan 35.3^\circ$$

$$= 47.6 kN/m^2$$

Alternatively the value of τ_{ff} could have been read directly from Fig. 8.19.

8.7.2 The Consolidated Undrained (CU) Test

The difference between this triaxial compression test and the consolidated drained test is that in the consolidated undrained test the soil is sheared under undrained conditions. This means that pore pressures may develop during shearing so that total and effective stress paths will not generally coincide.

Fig. 8.20 represents the results of two consolidated undrained tests on a soil. The initial consolidation stresses are represented by points A and B. The total stress paths (q vs. p) for the standard type of test in which σ_3 is maintained constant and σ_1 is increased, are represented by lines AC and BD. Possible effective stress paths (q vs. p') are shown by the dashed lines AE and BF. The total and effective failure Mohr circles have been drawn and the failure envelope to the effective circles will yield the effective stress parameters c' and ϕ'. These will not be the same as the total stress parameters which have been labelled c and ϕ.

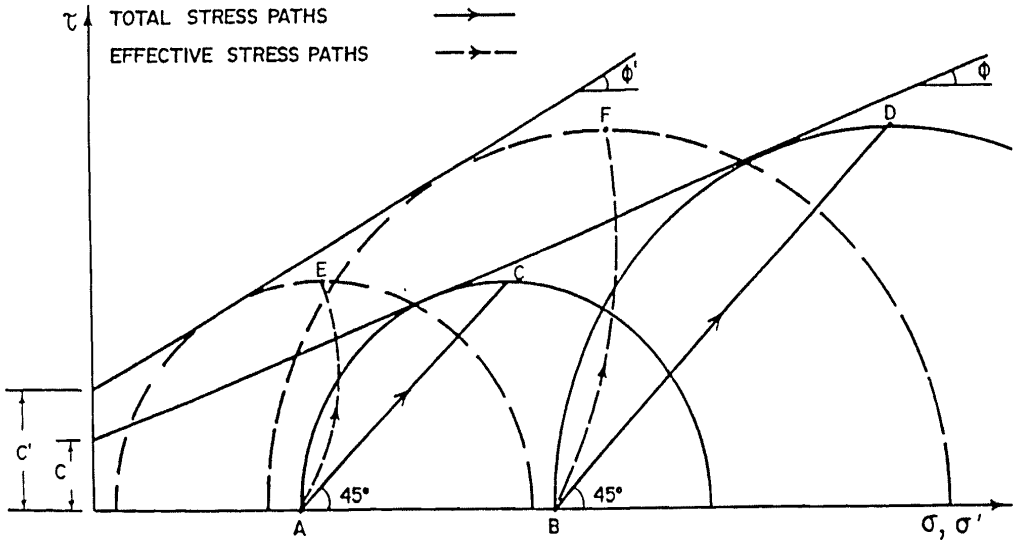

Fig. 8.20 Consolidated Undrained Tests

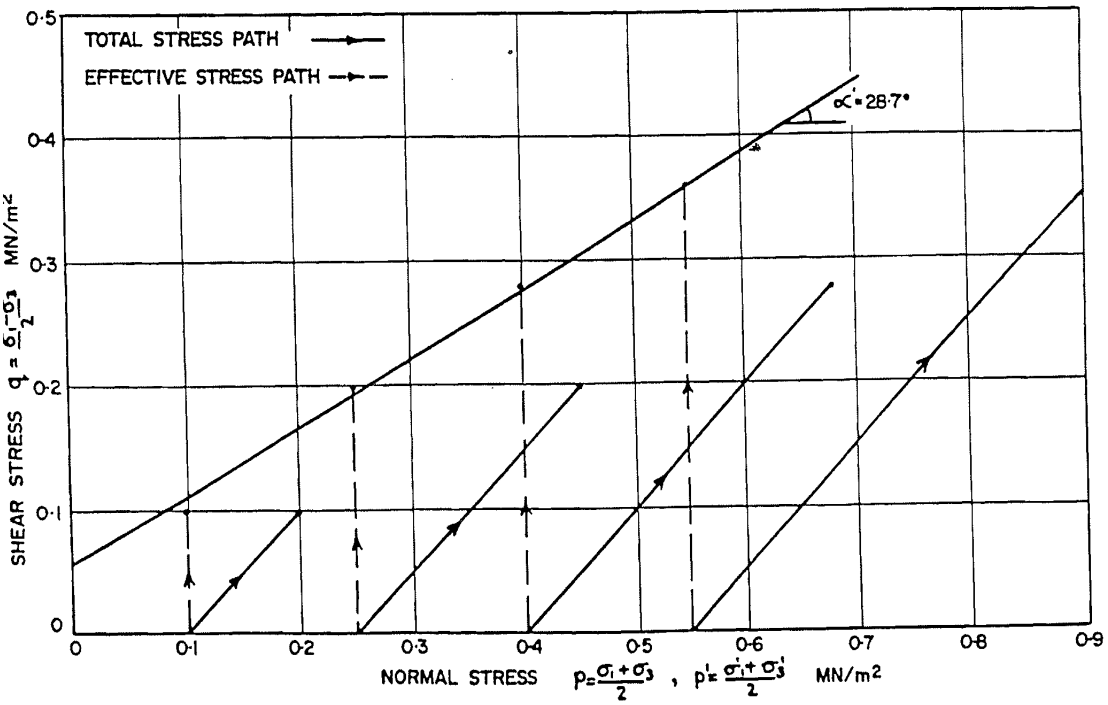

Fig. 8.21

The total stress parameters are found to be stress path dependent but the effective stress parameters are not. That is, if the triaxial compression test was conducted by varying both σ_1 and σ_3 the position of the total stress path would change but the position of the effective stress path would be substantially unchanged. In this non standard type of test the total stress parameters would differ from those obtained in the standard test but the effective stress parameters would be approximately the same as those obtained in the standard test illustrated in Fig. 8.20. As illustrated by the foregoing discussion it is commonly assumed that the effective stress parameters c' and ϕ' are soil constants whereas the total stress parameters c_{cu} and ϕ_{cu} are not soil constants but depend upon the stress path followed to failure.

As mentioned in section 8.7.1 the drained strength parameters c_d and ϕ_d are effective stress parameters. Consequently it would be expected that the effective stress parameters obtained from both drained and undrained tests will be equal. (Henkel, 1959). That is

$$\phi_d = \phi' \qquad c_d = c' \tag{8.18}$$

Approximate agreement between these parameters is supported by test data and this forms the basis of the common assumption that the effective stress and drained strength parameters are identical.

EXAMPLE

The following data was obtained from consolidated undrained tests on a soil for which, following consolidation, the sample was failed in the standard way by increasing σ_1 while keeping σ_3 constant.

Isotropic Consolidation Pressure (σ_c') (MN/m^2)	**Major Principal Stress at Failure (σ_{1f}) (MN/m^2)**
0.10	0.30
0.25	0.65
0.40	0.96
0.55	1.27

If the pore pressure parameters for this soil are A = 0.5, B = 1.0 determine the effective stress parameters c' and ϕ' without drawing the Mohr circles.

The values of c' and ϕ' may be found by means of a q - p plot as shown in Fig. 8.21. The total stress paths are shown by the full lines which commence at the consolidation stress on the horizontal axis and terminate at the failure values of q and p. The calculation of these values is illustrated for the first test

$$\sigma_{3f} = \sigma'_c = 0.10\text{MN/m}^2$$

$$\sigma_{1f} = 0.30\text{MN/m}^2$$

$$\therefore \quad p_f = \frac{\sigma_{1f} + \sigma_{3f}}{2} = \frac{0.30 + 0.10}{2}$$

$$= 0.20\text{MN/m}^2$$

$$q_f = \frac{\sigma_{1f} - \sigma_{3f}}{2} = \frac{0.30 - 0.10}{2}$$

$$= 0.10\text{MN/m}^2$$

The pore pressures at failure may be calculated by means of equation (7.9). For the first test

$$\Delta u = B\left[\Delta\sigma_3 + A(\Delta\sigma_1 - \Delta\sigma_3)\right]$$
$$= 1[0 + 0.5\ (0.20 - 0)]$$

$$= 0.10\text{MN/m}^2$$

$$\therefore \quad p_f' = p_f - \Delta u$$

$$= 0.20 - 0.10$$

$$= 0.10\text{MN/m}^2$$

This type of calculation enables the end point of the effective stress paths to be located. Since the A parameter is constant the effective stress path is a straight line. The effective stress paths are shown by the dashed lines in Fig. 8.21.

Through the end points of the effective stress paths a line of best fit has been sketched. The equation of this line is

$$q_f \quad - \quad a' + p_f' \tan \alpha'$$

where $a' = 0.055 MN/m^2$

$\alpha' = 28.7^\circ$

for which c' and ϕ' may be calculated by means of equations (8.17)

$$\phi' = \sin^{-1} (\tan \alpha')$$

$$= 33.2^\circ$$

$$c' = \frac{a'}{\cos \phi'} = 0.066 MN/m^2$$

8.7.3 The Unconsolidated Undrained (UU) Test

This test is carried out on a soil sample which has already been consolidated to some stress in the field or in the laboratory. The test is particularly significant in the case of saturated soil. The procedure in this test involves the application of a confining pressure (σ_3 or σ_c) under undrained conditions followed by the shearing of the soil under undrained conditions.

The results of three such tests on a saturated soil are illustrated in Fig. 8.22. OA represents the initial consolidation stress (σ_c'). The total confining pressures for the three tests are zero, OB and OC respectively. With a saturated soil a change in the confining pressure will result in the development of an equal pore pressure change. The pore pressures and effective stresses in the three soil samples prior to shearing are respectively:

(i) $\Delta u = \sigma_3 - \sigma_3' = O - OA = -OA$

$\sigma_3' = \sigma_3 - \Delta u = O - (-OA) = OA = \sigma_c'$

(ii) $\Delta u = OB - OA = BA$

$\sigma_3' = OB - BA = OA$

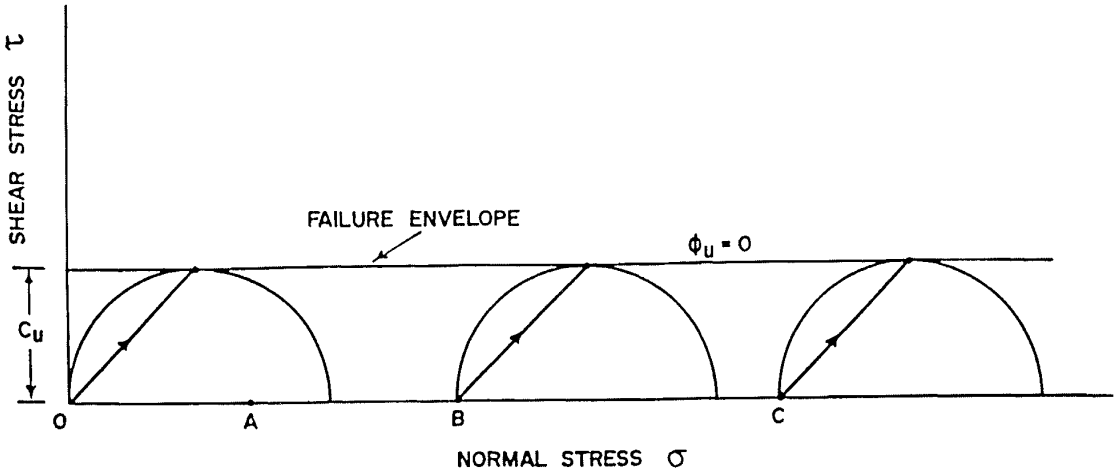

Fig. 8.22 Unconsolidated Undrained Tests on Saturated Soil

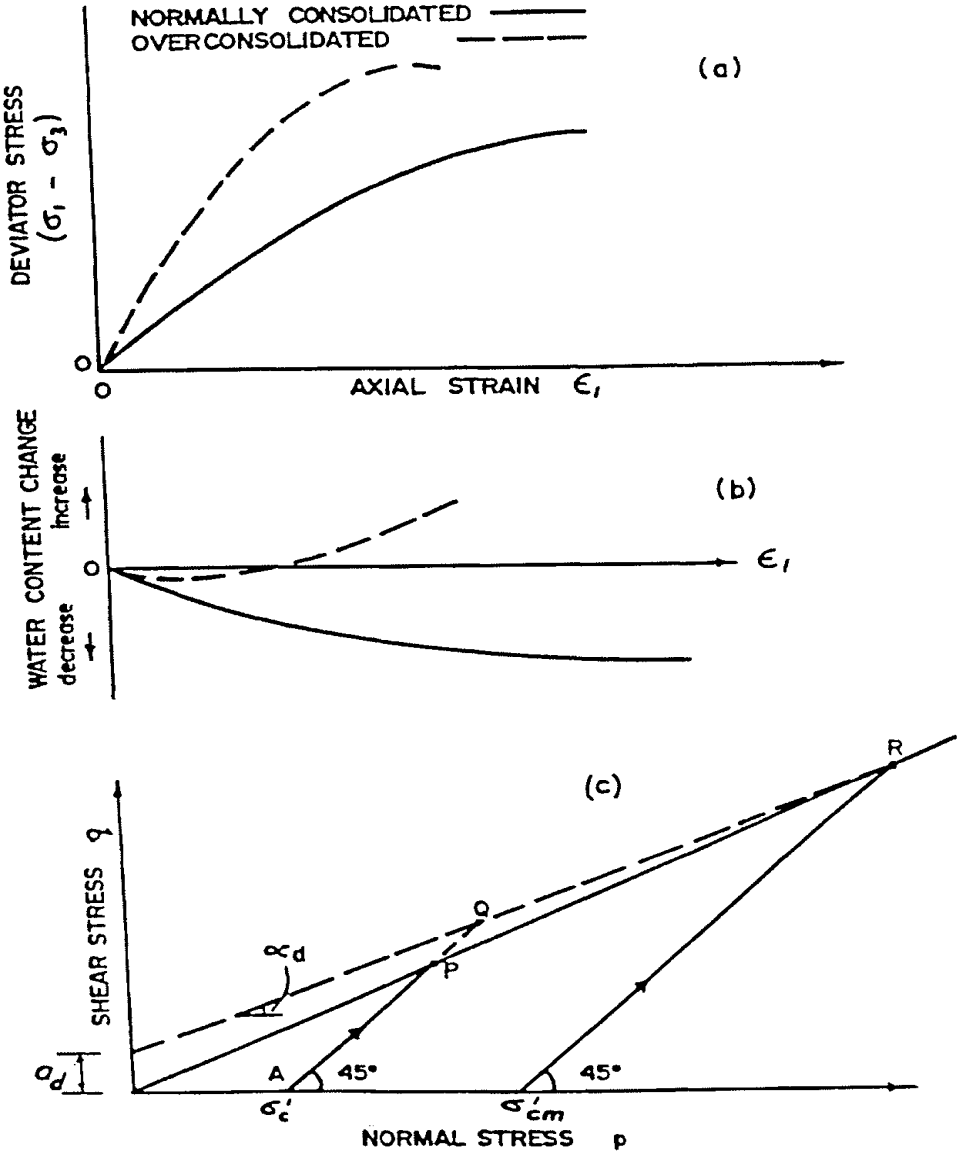

Fig. 8.23 Effect of Overconsolidation Upon Drained Strength

(iii) $\Delta u = OC - OA = CA$

$\sigma_3' = OC - CA = OA$

The first test, a special type of unconsolidated undrained test in which the confining pressure (σ_3) is zero, is known as the unconfined compression test as described in section 8.1. The failure value of σ_1 in this test is the unconfined compressive strength. As shown above the pre-shear value of the pore pressure is negative, that is, sub-atmospheric. If this pore pressure is sufficiently large numerically the pore water may cavitate.

The total stress paths have been drawn for the three tests in Fig. 8.22 and the tests have been carried out by increasing σ_1 while maintaining σ_3 (= σ_2) constant at the pre shear values of zero, OB and OC respectively. As also shown in Fig. 8.22 the failure circles for the three tests have the same size. This result is to be expected since the pre shear values of the effective confining pressures (σ_3') for all three samples are equal. This means that the failure envelope in terms of total stresses is horizontal, that is, $\phi_u = 0$. The only strength component in this type of test is the undrained cohesion c_u. It should be emphasised that $\phi_u = 0$ only when

(a) a saturated soil is subjected to an unconsolidated undrained test, and
(b) the results are expressed terms of total stresses.

Actually it is not possible to determine the effective stress parameters by means of this type of test as described above. To do so it is necessary to carry out a consolidated undrained test in which the pore pressures are measured.

The undrained cohesion c_u is closely related to the consolidation stress σ_c' (OA in Fig. 8.22). If the consolidation stress is increased then the resulting undrained cohesion is increased. It may be shown that for a soil in which c' = 0.

$$\frac{c_u}{\sigma'_c} = \frac{\sin \phi'}{1 + (2A_f - 1) \sin \phi'} \qquad (8.19)$$

where A_f is the pore pressure parameter A at failure.

Skempton (1957) has found that the values of (c_u/σ'_c) for normally consolidated marine clays increase with increasing plasticity index of the soils, (see Fig. 8.29). For normally consolidated clay deposits, he expressed the relationship as

$$(c_u/\sigma_c') = 0.11 + 0.0037 \ (PI) \qquad (8.20)$$

where PI is the plasticity index.

8.8 EFFECT OF OVERCONSOLIDATION ON SOIL STRENGTH

8.8.1 Drained Strength

During the shearing stage of a triaxial compression test a saturated normally consolidated soil (ie. one which has never been subjected to a consolidation stress higher than the one applied for the test) behaves in a way that is significantly different from that for an overconsolidated sample of the same soil. This difference in behaviour for consolidated drained tests is illustrated in Fig. 8.23. The normally consolidated sample has been consolidated to a stress σ_c' whereas the overconsolidated sample has been consolidated to a stress σ'_{cm} followed by a decrease of the consolidation stress to σ'_c.

The stress-strain behaviour shown in Fig. 8.23 (a) for these two samples indicated that the overconsolidated sample has a higher strength and fails at a smaller axial strain compared with the normally consolidated sample. The volume change behaviour for the two samples also differs substantially. This is illustrated by the water content changes in Fig. 8.23 (b). In this figure an increase in water content means an increase in volume of the sample. While the normally consolidated sample compresses throughout the test, the overconsolidated sample increases in volume following an initial decrease.

The stress paths for these two samples are shown by lines AP and AQ in Fig. 8.23 (c). The normally consolidated sample fails at point Q. If a number of tests were carried out (with the maximum consolidation stress for the overconsolidated samples equal to σ'_{cm}) the failure lines as shown would be obtained.

The equation for each of these lines would be of the form

$$q_f = a_d + p_f \tan \alpha_d$$

where q_f and p_f are the failure values of q and p

a_d and α_d are the drained strength parameters from the q - p plot for the particular soil

Comparing the two sets of strength parameters:

a_d (overconsolidated sample) > a_d (normally consolidated sample)

$$\alpha_d \text{ (O.C. sample)} \quad < \quad \alpha_d \text{ (N.C. sample)}$$

in fact the value of a_d (and the corresponding value of cohesion, c_d) for the normally consolidated sample is equal to or very close to zero for many soils.

The failure line for the overconsolidated sample terminates at point R in Fig. 8.23 (c) since the soil will be normally consolidated if the consolidation stress equals or exceeds the value of σ'_{cm} indicated in the figure. The foregoing discussion illustrates that overconsolidation of a soil increases the drained cohesion and decreases the drained angle of shearing resistance compared with the corresponding values for a normally consolidated soil.

8.8.2 Undrained Strength

The undrained strength behaviour for typical normally and overconsolidated saturated samples is illustrated in Fig. 8.24. In part (a) of the figure the stress-strain plot shows that the overconsolidated sample possesses a greater strength and fails at a smaller value of axial strain compared with the normally consolidated sample.

The pore pressure changes during the test are generally consistent with inferences which may be drawn from the volume change behaviour in the drained tests described in section 8.8.1. That is, if a volume increase occurs in the drained test during shearing, it might be expected that a pore pressure decrease would take place in the undrained test. These expectations are confirmed as shown in Fig. 8.24 (b). This plot shows that for the normally consolidated sample the pore pressures increase throughout the test, whereas the overconsolidated sample shows a pore pressure decrease after an initial increase. If these pore pressure changes are expressed in terms of the pore pressure parameter A, the changes throughout the test are as shown in Fig. 8.24 (c). At failure, the normally consolidated sample gives a value of the A parameter (A_f) in the vicinity of unity, a common occurrence with normally consolidated soil, whereas the overconsolidated sample gives a negative A_f value in this example.

It is found that for a particular soil the A_f value varies systematically with the overconsolidation ratio (ratio of σ'_{cm} to σ'_c). A typical relationship is shown in Fig. 8.25 which shows the A_f value passing through zero at an overconsolidation ratio in the region of 4.

Typical stress paths for both normally and overconsolidated samples are shown in Fig. 8.26. Point A represents the consolidation stress (σ'_c) from which the stress paths commence. For the normally consolidated sample the total stress path is represented by AC and the corresponding effective stress path is AB which is plotted from a knowledge of the measured pore pressures throughout the test. From the results of several such tests the failure line (full line) through point B may be found.

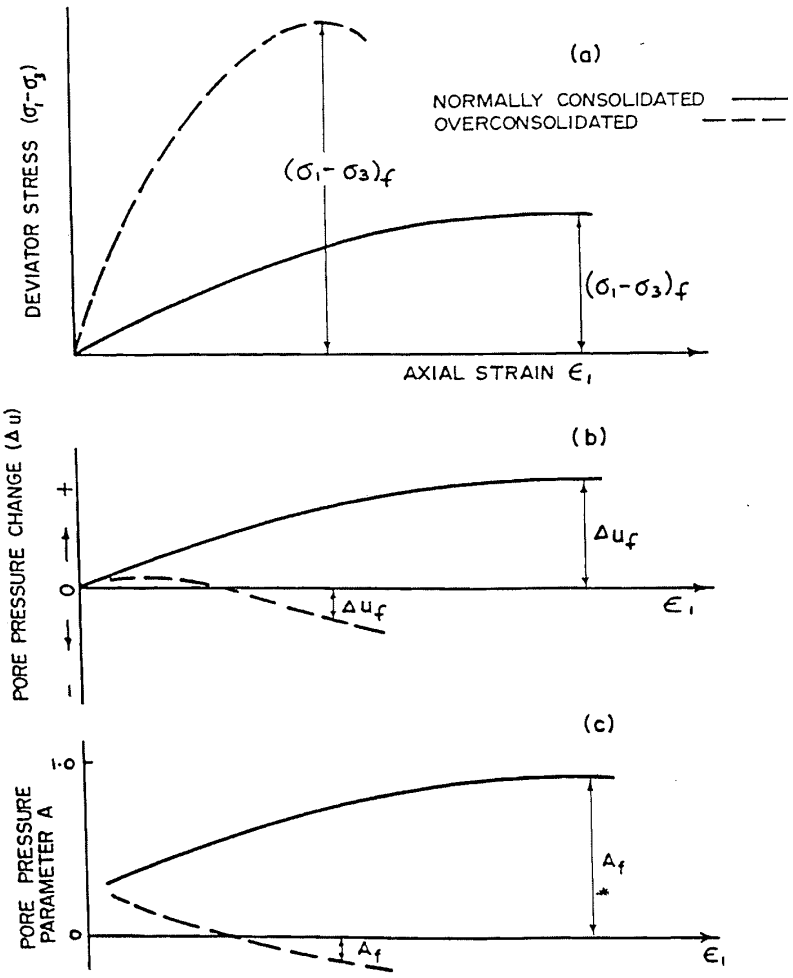

Fig. 8.24 Effect of Overconsolidation Upon Undrained Strength

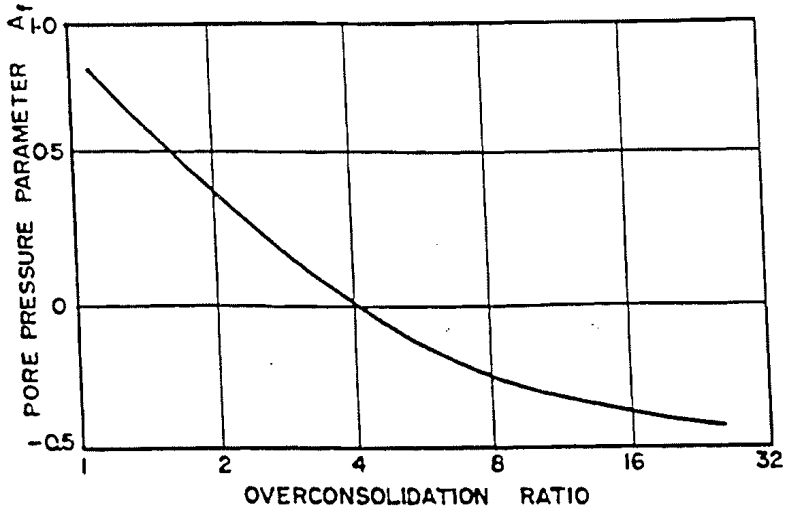

Fig. 8.25 Effect of Overconsolidation on Pore Pressure Development

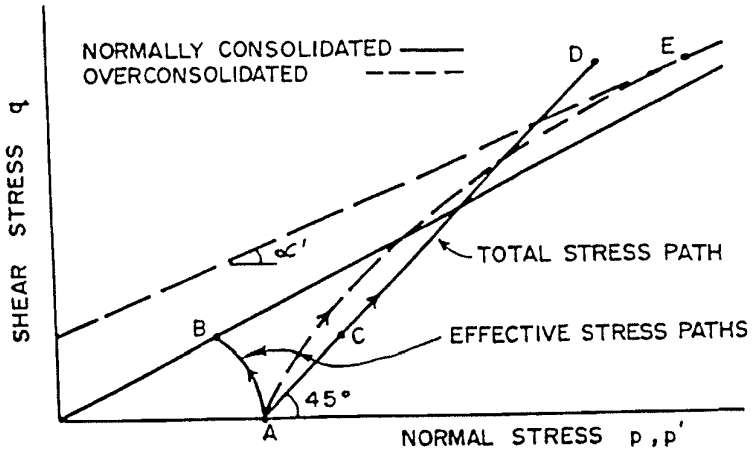

Fig. 8.26 Effect of Overconsolidation on Stress Path

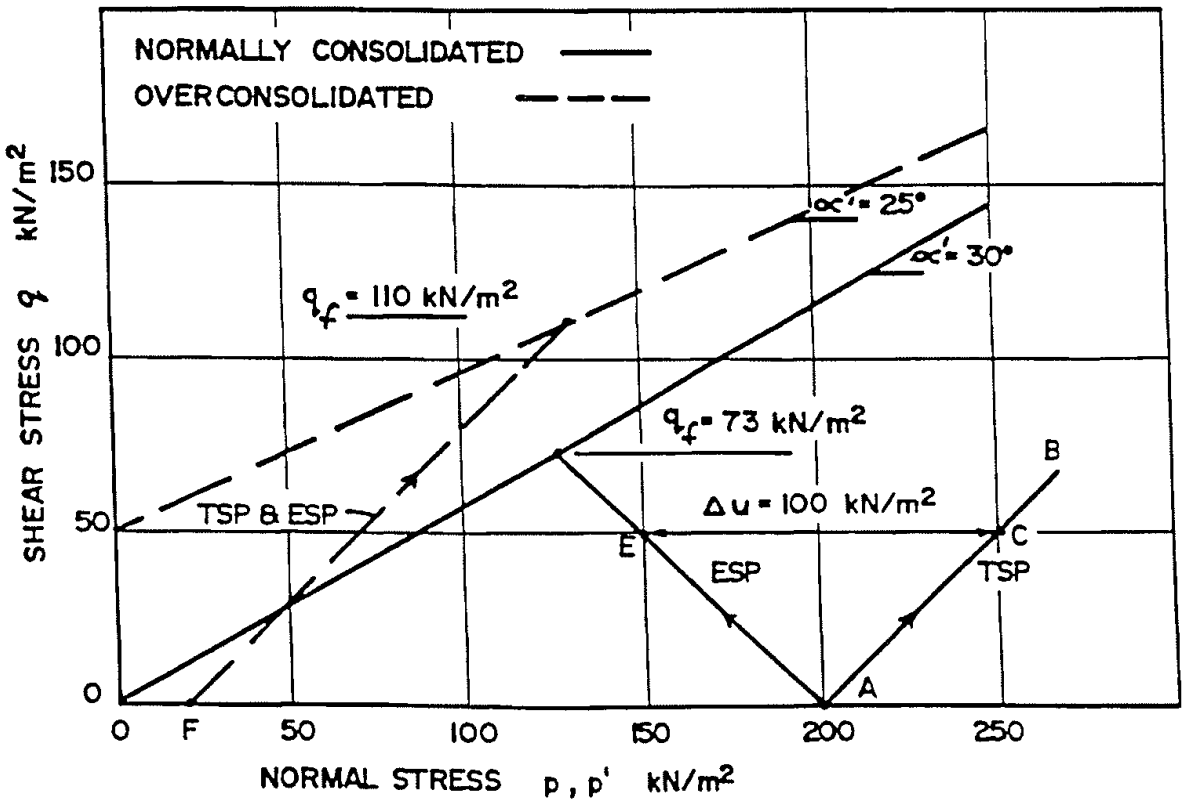

Fig. 8.27

For the overconsolidated sample the total stress path is AD and the effective stress path is AE. These two paths cross when the pore pressure becomes zero. The dashed line represents the failure line obtained from the results of several tests (using the same value of σ'_{cm} but different values of σ'_c).

The equation of both failure lines in Fig. 8.26 is of the form

$$q_f = a' + p_f' \tan \alpha'$$

where a' and α' are the effective stress parameters.

These strength parameters for the normally and overconsolidated samples are approximately equal to the corresponding drained strength parameters a_d and α_d. This means that the comparison between the drained strength parameters given in section 8.8.1 also applies to the effective stress parameters. It also means that a' (and c') for normally consolidated soils are approximately equal to zero. (see Henkel, 1960).

EXAMPLE

Determine the shear strengths (in terms of q_f) for the following two cases in which standard consolidated undrained tests are performed (σ_1 increased to failure) on saturated soils.

(a) A normally consolidated soil for which a' = 0, α' = 30°, A = 1.0, is consolidated isotropically to a stress of 200kN/m^2,

(b) An overconsolidated soil for which a' = 50kN/m^2, α' = 25°, A = 0.0 is finally consolidated isotropically to a stress of 20kN/m^2.

(a) This problem can be solved most simply by drawing stress paths. The total stress path will lie in the direction of AB as shown in Fig. 8.27. The effective stress path can be drawn if the pore pressure changes are known. As A is given as a constant the effective stress path will be a straight line commencing at point A. One other point on the line will locate its direction. The pore pressure changes may be calculated from

$$\Delta u = B\left[\Delta\sigma_3 + A\left(\Delta\sigma_1 - \Delta\sigma_3\right)\right]$$

$$= A\,\Delta\sigma_1 \text{ since } B = 1 \text{ for a saturated soil and } \Delta\sigma_3 = 0$$

$$= \Delta\sigma_1$$

For a value of $\Delta\sigma_1$ of 100kN/m^2 the value of Δu at this stage of the test is therefore equal to 100kN/m^2. At this point

$$p = 200 + \frac{100}{2} = 250\text{kN/m}^2$$

$$q = \frac{100}{2} = 50\text{kN/m}^2$$

which is represented by point C in Fig. 8.27.

The corresponding effective stress point is therefore located at point E. Line AE now establishes the direction of the effective stress path. This line is now continued until it intersects the failure line at a value of q_f of 73kN/m^2.

(b) For the overconsolidated soil the total stress path commences at point F as shown on Fig. 8.27 and extends upwards to the right as indicated. To find the effective stress path the pore pressure changes must be calculated

$$\Delta u = B\left[\Delta\sigma_3 + A(\Delta\sigma_1 - \Delta\sigma_3)\right]$$

$$= A\Delta\sigma_1$$

$$= 0$$

Since there are no pore pressure changes throughout the test the total and effective stress paths coincide. So the stress path shown by the dashed line in Fig. 8.27 is simply extended until it intersects the failure line at a value of q_f of 110kN/m^2.

REFERENCES

Bieniawski, Z.T., (1968), "The effect of specimen size on compressive strength of coal", Int. J. Rock Mech. Min. Sci., Vol. 5, pp. 325-335.

Bieniawski, Z.T., (1974), "Estimating the strength of rock materials", Journal of the South African Inst. of Mining and Metallurgy, Vol. 74, pp. 312-320.

Bieniawski, Z.T. and Van Heerden, W.L. (1975), "The significance of in-situ tests on large rock specimens", Int. J. Rock Mech. Min. Sci., Vol. 12, pp. 101-113.

Bishop, A.W., (1966), "The Strength of Soils as Engineering Materials", Geotechnique, Vol. 16, pp. 91-130.

Bishop, A.W., and Bjerrum, L., (1960), "The Relevance of the Triaxial Test to the Solution of Stability Problems", Research Conf., on Shear Strength of Cohesive Soils, Colorado, pp 437-501.

Bishop, A.W., and Henkel, D.J., (1962), "The Measurement of Soil Properties in the Triaxial Test", Edward Arnold Ltd., 228 p.

Bjerrum, L., (1954), "Geotechnical Properties of Norwegian Marine Clays", Geotechnique, Vol. 4, pp. 49-69.

Brown, E.T. (Ed.), (1981), "Rock Characterization Testing and Monitoring, ISRM Suggested Methods", Pergamon Press Ltd., Oxford, 211 p.

Franklin, J.A. and Dusseault, M.B. (1989), "Rock Engineering", McGraw Hill Inc., 600p.

Goodman, R.E., (1980), "Introduction to Rock Mechanics", John Wiley & Sons, New York, 478p.

Henkel, D.J., (1959), "The relationship between the strength, pore water pressure and volume change characteristics of saturated clays", Geotechnique, 9, 119-135.

Henkel, D.J., (1960), "The Shear Strength of Saturated Remoulded Clays", Research Conf. on Shear Strength of Cohesive Soils, Colorado, pp 533-554.

Hoek, E. (1968) "Brittle failure of rock", in K. Stagg and O. Zienkiewicz (eds.), Rock Mechanics in Engineering Practice, Wiley, New York.

Hoek, E. and Brown, E.T., (1980), “Empirical Strength Criterion for Rock Masses”, J. Geotech. Eng. Div., ASCE,, Vol. 106, No. GT9, pp 1013-1035.

Jaeger, J. and Cook, N.G.W. (1976), “Fundamentals of Rock Mechanics”, Second Ed., Chapman and Hall, London.

Jahns, H. (1966), “Measuring the strength of rock in-situ at an increasing scale”, Proc. 1st Cong. ISRM (Lisbon), Vol. 1, pp 477-482.

Johnston, I.W., (1985), “The Strength of Intact Geomechanical Materials”, J. Geotech. Eng. Div., ASCE, Vol. 111, No. 6, pp 730-749.

Kenney, T.C., (1959), Discussion, Jnl. Soil Mechanics and Foundations Division, ASCE, Vol. 85, No. SM3, pp 67-79.

Lambe, T.W., and Whitman, R.V., (1979), “Soil Mechanics, SI Version”, John Wiley & Sons, Inc., 553p.

Marsland, A. (1971), “The Use of In-Site Tests in a Study of the Effects of Fissures on the Properties of Stiff Clays”, Proc. First Aust. - N.Z. Conf. on Geomechanics, Melbourne, Vol. 1, PP180-189.

Mitchell, J.K., (1976), “Fundamentals of Soil Behaviour”, John Wiley & Sons, Inc., 422 p.

Olson, R.E., (1974), “Shearing Strength of Kaolinite, Illite and Montmorillonite”, Jnl. of the Geotechnical Division, ASCE, Vol. 100, No. GT 11, pp 1215-1229.

Pratt, H.R., Black, A.D., Brown, W.D. and Brace, W.F., (1972), “The effect of specimen size on the mechanical properties of unjointed diorite”, Int. J. Rock Mech. Min. Sci., Vol. 9, No. 4, pp 513-530.

Skempton, A.W., (1957), Discussion on “The Planning and Design of the New Hong Kong Airport”, Proc. Instn. Civ. Engrs., London, 7, pp 305-307.

Terzaghi, K. and Peck, R.B., (1967), “Soil Mechanics in Engineering Practice”, John Wiley & Sons, New York, 729 p.

Vutukuri, V.S., Lama, R.D. and Saluja, S.S., (1974), “Handbook on Mechanical Properties of Rocks”, Vol. 1, Trans Tech Publications, 280p.

Yudhbir, L.W. and Prinzl, F. (1983), “An Empirical Failure Criterion for Rock Masses”, Proc. 5th Int. Cong. Rock Mech., Melbourne, Vol. B, pp 1-8.